



Photon momentum change of quasi-smooth solar sails

D. ZOLA,^{1,*} C. CIRCI,² G. VULPETTI,³ AND S. SCAGLIONE¹

¹ENEA, Centro Ricerche della Casaccia, Via Anguillarese 301, 00123 Roma, Italy

²Department of Astronautical, Electrical and Energy Engineering, Sapienza University of Rome, Via Salaria 851, 00138 Rome, Italy

³International Academy of Astronautics, Paris 75766, France

*Corresponding author: danilo.zola@enea.it

Received 21 February 2018; revised 6 June 2018; accepted 6 June 2018; posted 7 June 2018 (Doc. ID 324591); published 5 July 2018

The solar photon sail (SPS) allows space missions without propellant that would otherwise not be feasible. Thrust models frequently used in the literature for the calculation of trajectories often underestimate the effect that the surface roughness has on SPS dynamics. A small variation of the thrust vector can induce a large modification of sail flight. In this work, the variation of the photon momentum vector (PMV) is computed as resulting from the incident Sun radiation, taking into account the absorbed and reflected photons. The momentum resulting from diffuse light has been modeled by using vectorial scattering theories in the limit of a quasi-smooth sail where the first-order of Rayleigh–Rice can be applied. In particular, the momentum change resulting from diffuse radiation causes a PMV reduction as well as a deviation of its direction from what is foreseen in the case of an ideally smooth sail. © 2018 Optical Society of America

OCIS codes: (260.2110) Electromagnetic optics; (240.5770) Roughness; (290.0290) Scattering.

<https://doi.org/10.1364/JOSAA.35.001261>

1. INTRODUCTION

The solar photon sail (SPS) allows continuous low-thrust in-space propulsion with no propellant consumption, thus providing a wide range of opportunities for high-energy and low-cost missions, many of which would be impracticable by conventional rocket spacecraft [1–4]. As a point of fact, a high-orbital-energy mission requires large speed changes with corresponding massive propellant consumption, large tanks, high subsystem complexity, a high number of propulsive or gravity-assist maneuvers, and a long flight time duration [2,3]. Ultimately, the spacecraft mission's reliability would decrease or would be restricted to a narrow launch window; in any case, the mission's cost could become prohibitive. The precision and the accuracy of SPS spacecraft trajectory design depends also on the physical model of the interaction between the (solar) photon flux and the sail surface. Even model uncertainties equal to or larger than the total solar irradiance (TSI) fluctuation (or about 0.1% of the mean) in the calculation of the thrust vector may entail a mission failure (Section 6.5.7 in Ref. [4]). Moreover, knowledge of the thrust phenomena allows the design of sailcraft guidance systems able to correct trajectory errors also due to unpredictable solar events during the flight. For these reasons, it is important to work on accurate models that can upgrade the most common ones used hitherto in the literature, e.g., those in Refs. [2,3,5,6].

The so-called ideal sail model, where the sail is assumed to be like a perfect mirror, is very straightforward, and it is useful for explaining some basic properties and features such as characteristic acceleration, lightness number, sail loading, and solar radiation pressure [2]. Since the specular reflection (R_s) is 100% of the incident light, the resultant sail's thrust is along the sail's surface normal pointing outwards the Sun. This model is used for preliminary mission analysis, assuming that realistic thrust can be obtained, reducing the SPS performance. This assumption is very optimistic, and the real sail thrust is very far from the modeled one; this could lead to uncorrectable differences between the designed trajectory and the actual one [7]. Considering that the thrust is due to the interaction between incident light and the surface, more detailed models have to be taken into account, including more realistic optical features of the surface, since the Sun's incident light is actually specularly and diffusely reflected as well as partially absorbed and re-emitted. In thrust models, some of the parameters are the mean spectral absorptance and reflectance, both diffuse and specular, weighted on the photon flux from the Sun.

The so-called optical force model of the sail's thrust [3] includes the sail's diffuse reflectance, but it does not relate the optical parameters to the roughness of the sail surface; thus, one often has to resort to average parameters taken from the literature. This model assumes that the sail is flat, the surface

roughness effect is considered through empirical parameters as a non-Lambertian coefficient (χ), and the mean reflectance does not depend on the light incidence angle. In particular, the model assumes that the diffuse radiation is distributed around the direction of SPS normal. Although the model predicts that the angle between the total momentum of the sail and the SPS normal is not null (the so-called centerline angle), it does not take into account that diffuse radiation is mostly widespread for angles close to the specular direction. The consequence can be an overestimation of the SPS centerline angle. Finally, a more accurate model—for computing the sail-craft lightness vector function (which is proportional to the thrust acceleration), introduced by Vulpetti [4]—no longer assumes the photon momentum due to the diffuse reflection along the SPS normal. Nevertheless, the model still needs accurate estimation of the optical parameters for the computation of SPS trajectory. For these reasons, light scattering theories cannot be ignored.

At first glance, estimation of the diffuse radiation appears to be the most important improvement in this framework. Total integrated scatter (TIS) [8,9] can be first used in order to better take into account the effect of roughness on the sail's optical properties. TIS relates the spectral hemispherical diffuse reflectance R_D of a surface to a single finish parameter, which is its root mean square (rms) roughness \tilde{z} . TIS is given by the ratio between the spectral hemispherical diffuse reflectance, $R_D(\lambda)$, and the spectral hemispherical reflectance $R_T(\lambda)$ (also called total reflectance in the literature) [10], i.e., it is the fraction of the diffuse spectral power related to the total reflected spectral power,

$$\text{TIS} = \frac{R_D}{R_T} = 1 - \exp \left[- \left(\frac{4\pi\tilde{z} \cos \theta_i}{\lambda} \right)^2 \right]. \quad (1)$$

However, the TIS expression is valid if \tilde{z} is at least 10 times less than λ . In 1999, Vulpetti and Scaglione [11] suggested utilizing TIS for the computation of SPS thrust. Although TIS results in a more accurate model for evaluating the scattering effect on the sail's thrust, it does not resolve the angular distribution of the diffused light and neglects its polarization. The former is crucial for calculating the moment direction, and the latter is important if the Sun's radiation incidence angle θ_i is far from the sail normal ($\hat{\mathbf{m}}$, taken in the direction of the Sun) [12]. For this reason, TIS was used for a refined computation of the parameters in the optical force model [11,13,14].

In order to actually take into account the scattering phenomenon, one has to switch to vector scattering theory (VST), which allows a direct calculation of the photon momentum change, including also the light polarization. The Rayleigh–Rice theory [15] (RRT) was the first VST to be employed for this purpose at a theoretical level [4]. Many of the phenomena entering the SPS thrust were analyzed quantitatively in Ref. [4], though Ref. [16] focused only on the R_D contribution to thrust as owing to the sail's surface roughness. Nevertheless, and notably, surface roughness also affects the sail's spectral absorptance (A), and it subtracts radiative power to the sail's spectral hemispherical reflectance (R_T). The estimation of light absorbed and diffused are both related to scattering theories.

In this work, the change of total photon momentum \mathbf{D} [17] is computed by using VST theories, one of these properly suitable for computing absorptance. In this way, taking into account the effects of surface roughness on absorbed, specularly reflected, and diffuse radiation, the photon momentum vector (PMV) as a function of incidence angle of the Sun's radiation is computed. In the following section, the different contributions to PMV are reviewed; then in Section 3 the case of a smooth aluminized sail is discussed. The absorptance due to the surface roughness is discussed in Section 4. Finally, in Section 5, the PMV change is computed for SPS with a quasi-smooth surface.

2. MOMENTUM CHANGE OF PHOTONS INTERACTING WITH SPS

The photon momentum change \mathbf{D} per time and area unit as a function of the surface roughness, generated by incoming and reflected photons, is measured in pascals (Pa), and it is related to radiation pressure. The momentum \mathbf{D}_r , given by the reflected photons both specularly as well as diffusively scattered, is given by

$$\mathbf{D}_r(\theta_i) \equiv \frac{1}{c} \int_{\lambda_{\min}}^{\lambda_{\max}} I_d(\lambda) d\lambda \int_{\Omega_s} \cos \theta_s \text{BRDF}(\epsilon, h; \lambda, \theta_i, \theta_s, \phi_s) \hat{\mathbf{d}}_s d\Omega_s. \quad (2)$$

In Eq. (2), c is the speed of light in a vacuum, and $I_d(\lambda)$ is the photon flux (measured as $\text{W nm}^{-1} \text{m}^{-2}$), which is a function of wavelength λ and depends on the distance from the Sun and crossing $d\mathbf{S}_\perp$, the infinitesimal surface perpendicular to the photons' flux. λ_{\min} and λ_{\max} limit the spectral range where the irradiance is not negligible. The standard spectral range is from $\lambda_{\min} = 0.5 \text{ nm}$ to $\lambda_{\max} = 10^6 \text{ nm}$ [18]. Considering only the spectral Sun irradiance related to the range usually covered in optics, in our case, $\lambda_{\min} = 200 \text{ nm}$ and $\lambda_{\max} = 20000 \text{ nm}$. BRDF is the bidirectional reflection distribution function, defined as the ratio between the differential radiance and the differential irradiance [19]. BRDF is usually a function of the complex dielectric function of the sail's reflective layer, $\epsilon(\lambda, T)$, which depends on λ and temperature T . Moreover, BRDF depends on a statistical function h representing the surface morphology. Although it is not explicit in Eq. (2), BRDF depends on the polarization of source and reflected radiation. Finally, BRDF is a function of λ , incident angle θ_i , out-of-plane scattering angle θ_s , and in-plane scattering angle ϕ_s . The three angles are defined according to Fig. 1. Moreover Ω_s is the scattering solid angle, and $\hat{\mathbf{d}}_s$ is the unit vector of the scattered photon momentum,

$$\hat{\mathbf{d}}_s = (\sin \theta_s \cos \phi_s, \sin \theta_s \sin \phi_s, \cos \theta_s). \quad (3)$$

For $\theta_s = \theta_i$ and $\phi = 0$, the versor $\hat{\mathbf{d}}_s = \hat{\mathbf{d}}_r$ locates the specular direction. \mathbf{D}_r , induced by the incoming sunlight irradiance at θ_i , can be estimated if the BRDF of the sail is known for any $\lambda, \theta_s, \phi_s$.

For a distance from the Sun ρ_s such that it is a point source, $I_d(\lambda) = \text{SSI}(\lambda)/d^2$, where $d = \rho_s/\rho_{S-E}$, SSI is the Sun spectral irradiance, and $\rho_{S-E} = 1 \text{ AU}$ is the mean Sun–Earth

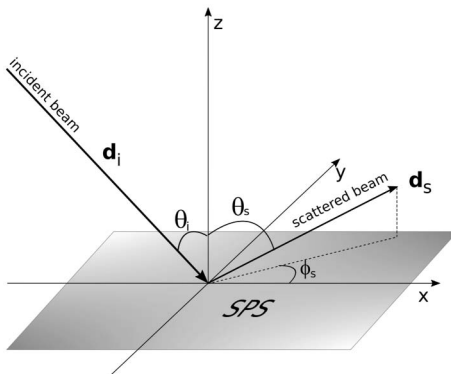


Fig. 1. Scattering geometry for defining the main angles and versors used in the text.

distance. In this work, ρ_S is assumed to be 1 AU, and in this case, $I_d(\lambda) \equiv I(\lambda)$.

The incoming radiation is also partially absorbed by the sail, and the *solar directional total absorptance* a weighted on $I(\lambda)$ is given by

$$a(\theta_i) = (1/\text{BSI}) \int_{\lambda_{\min}}^{\lambda_{\max}} A(\lambda, \theta_i) I(\lambda) d\lambda, \quad (4)$$

where $A(\lambda, \theta_i)$ is the *directional spectral absorptance* and the broad solar irradiance (BSI)

$$\text{BSI} = \int_{\lambda_{\min}}^{\lambda_{\max}} I(\lambda) d\lambda. \quad (5)$$

$\text{BSI} = 1365.94 \text{ W/m}^2$ at a 1 AU distance from Earth. $\text{BSI} \cong \text{TSI} = 1366.15 \text{ W/m}^2$, i.e., the total Sun irradiance, given by

$$\text{TSI} = \int_{0.5 \text{ nm}}^{10^6 \text{ nm}} I(\lambda) d\lambda, \quad (6)$$

and $\text{BSI}/c \cong \text{TSI}/c = 4.56 \mu\text{Pa}$ is the Sun's radiation pressure at 1 AU [20]. The major source of error is not due to the use of BSI instead of TSI but to the daily variation of SSI [21], especially for missions where the spacecraft moves close to the Sun.

The photon momentum change \mathbf{D} for the time and area unit resulting from the reflecting SPS is therefore given by

$$\mathbf{D} = \mathbf{D}_r - \mathbf{D}_i, \quad (7)$$

where \mathbf{D}_i is the momentum of the incoming photons,

$$\mathbf{D}_i = \frac{W(\rho)}{c} \hat{\mathbf{d}}_i, \quad (8)$$

and

$$\hat{\mathbf{d}}_i = (\sin \theta_i, 0, -\cos \theta_i). \quad (9)$$

W is the energy flux at a distance ρ_s from the Sun, and in this work $W = \text{BSI}/c$ is assumed.

In Fig. 2, an illustration of the momentum vectors \mathbf{D}_i and \mathbf{D} is shown. In the same figure, the momentum vectors \mathbf{D}_{rd} and \mathbf{D}_{rs} are also reported and respectively related to the diffuse and specularly reflected photons. Both of them are discussed in the following sections. Furthermore, θ_D and θ_C are respectively the

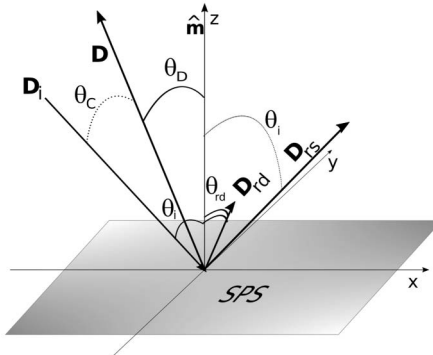


Fig. 2. Illustration of the momenta vectors and main angles discussed in this work. \mathbf{D}_{rs} , \mathbf{D}_{rd} are the photons' momenta due to the reflected and diffuse photons, respectively, discussed afterward in the paper.

centerline angle and the cone angle, whereas θ_{rd} is the angle formed by \mathbf{D}_{rd} with the sail normal $\hat{\mathbf{m}}$.

In Eq. (7), the momentum due to the photons emitted by the sail is neglected in this discussion. In this case, a sail with the front and back sides both aluminized at the same temperature is taken into account. In this introductory paper, we do not consider how ϵ changes with the temperature T , although metals change their optical properties on T [22,23]. The sail temperature, assumed in this work, is the room temperature (300 K) because $\epsilon(\lambda, 300 \text{ K})$ is used in our computations. Moreover, 300 K is close to the temperature of a self-standing aluminum sail (~ 330 K) orbiting about the Sun at 1 AU [3]. The Sun is supposed to be a point-like source of electromagnetic radiation, a very good assumption for 1 AU orbits [3,4]. Furthermore, all the optical quantities evaluated below refer to the beginning of a sail mission, namely, at the time of the sail's deployment operation. Therefore, we neglect the possible modification to the sail's absorptance (and to the ensuing reflectance change), caused by the protons and the α -particles of the solar wind, as their energy deposition on the sail increases with time.

PMV change can be used to calculate the force acting on the sail of surface S when the solar radiation is incoming on the sail with a pitch angle θ_i ,

$$\mathbf{f} = -\mathbf{D} S \cos(\theta_i). \quad (10)$$

The authors remark that in this work, the physical quantity expressed by the symbol \mathbf{D} and measured with Newton per meter squared (N/m^2) units is interpreted as the momentum of the photons' crossing during the time dt on the infinitesimal surface $d\mathbf{S}_\perp$ perpendicular to the photons' flux. Adopting this definition, the intensity of incident photon momentum D_i is independent of θ_i . On the other hand, the intensity of the momentum of reflected photons depends on θ_i because the optical properties of SPS, like reflectance, depend on θ_i . Since $d\mathbf{S}_\perp = d\mathbf{S} \cos(\theta_i)$, the force acting on SPS is given by Eq. (10). In Vulpetti's paper [16], the photon momentum \mathbf{D} includes the factor $\cos(\theta_i)$ because the photons' flux per area unit, crossing an infinitesimal SPS surface dS , is considered there. This means that the definition of \mathbf{D} in Ref. [16] corresponds to \mathbf{f}/S in this paper.

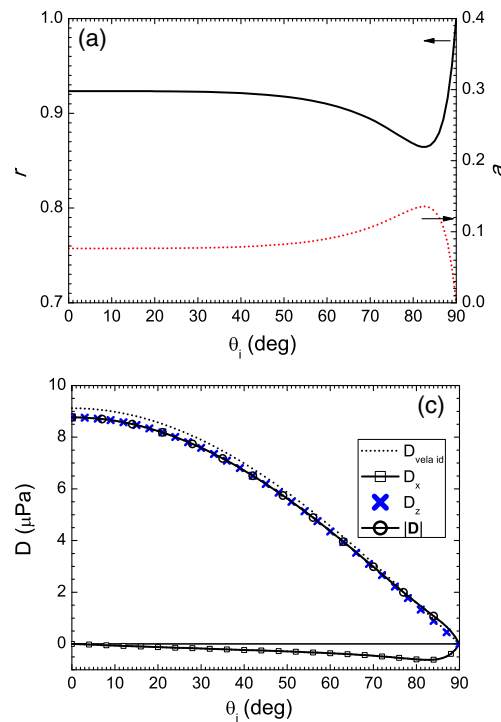
In this paper, the optical quantities are defined with a preference for the “*ance*” suffix over the “*ivity*” one. The definition of the optical quantities follows the nomenclature that distinguishes the source (solar, lamp) direction of the incoming radiation (directional, conical, or hemispherical), wavelength dependence (spectral), or if they are mean weighted on the spectral irradiance (total), and finally the direction of the emerging beam (directional, conical, or hemispherical) [24]. In this paper, the source is always the Sun, whereas the incoming radiation is always assumed to be collimated (directional). If the optical quantities do not depend on the type of source, then it is not mentioned. Moreover, the specular reflectance is not mentioned directionally for the emerging beam. The solar-radiation incidence is ($\phi_i = \pi, \theta_i$), as usually considered in a wave scattering problem.

3. SMOOTH ALUMINIZED SAIL

The computation of PMV change in the case of a smooth reflecting surface is largely discussed in the literature [2,3]. Here, the subject is reported in order to better explain the methods used and the following results reported in this paper. In order to unburden the discussion, many of the equations used in the work are reported in Appendix A.

In the case of a smooth sail that reflects the incident radiation only in a specular direction, the BRDF is given by

$$\text{BRDF}_S = \frac{R_S(\lambda, \theta_i)}{\cos \theta_i \sin \theta_i} \delta(\theta_i - \theta_s) \delta(\phi_s). \quad (11)$$



R_S is the *directional spectral specular reflectance*, and it is given by Fresnel laws [reported in Appendix A, Eq. (A8)]. R_S depends on the complex dielectric function $\epsilon(\lambda)$ of the reflecting material of the sail. In the case of a perfectly smooth sail coated with an aluminum film 100 nm thick, a fraction of the incident radiation is absorbed, but more than 90% of the incident radiation is reflected specularly. The *solar directional total specular reflectance* $r_s(\theta_i)$ is defined in a way analogous to a ,

$$r_s(\theta_i) = (1/\text{BSI}) \int_{\lambda_{\min}}^{\lambda_{\max}} R_S(\lambda, \theta_i) I(\lambda) d\lambda, \quad (12)$$

where $\epsilon(\lambda)$ is, in our case, the experimental complex function of a 100 nm thick aluminum film deposited by physical vapor deposition (PVD). More strictly, oxide a few nanometers thick naturally forms on aluminum surfaces when they are exposed to air. The optical indices of the oxide should also be considered, but they will be overlooked in this work.

In Fig. 3(a), the solar directional total specular reflectance (r_s) and solar directional total absorptance (a) of smooth SPS are reported as a function of θ_i . It is clearly demonstrated that r_s of the solar sail is far from 100%. The minimum in r_s at approximately 82° is due to the pseudo-Brewster angle due to the light polarization effects. The momenta \mathbf{D}_r and \mathbf{D}_i are reported in Fig. 3(b) for all the incident angles. The computation for \mathbf{D}_r was performed via BRDF by using Eq. (2) instead of using the classical equation, $\mathbf{D}_r = (\text{BSI}/c)r_s(\theta_i)(\sin \theta_i \hat{\mathbf{x}} + \cos \theta_i \hat{\mathbf{m}})$. In Fig. 3(b), the x and out-of-plane components of \mathbf{D}_r are plotted together with its modulus $|\mathbf{D}_r|$. Moreover, in the same graph, as dashed lines, the two components

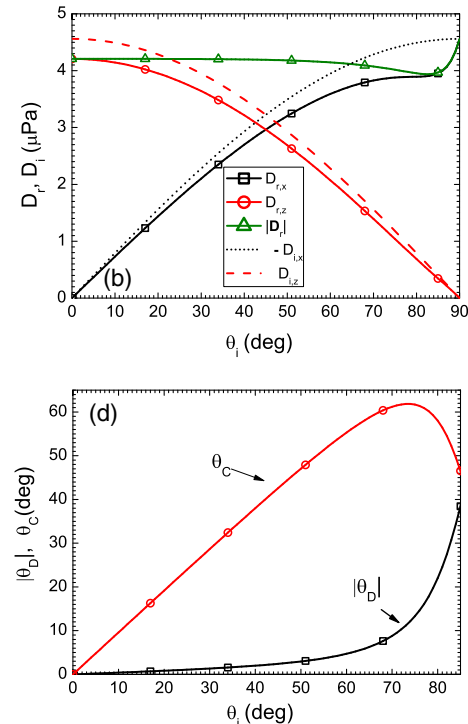


Fig. 3. (a) Solar directional total specular reflectance and solar directional total absorptance of a smooth aluminum SPS as a function of θ_i . (b) x, z components of the photon momentum, \mathbf{D}_r , due to the sunlight, specularly reflected. In the same panel, the module of \mathbf{D}_r is reported, and the x, z components of \mathbf{D}_i . (c) x, z , and module of the photon momentum change \mathbf{D} of SPS. (d) Centerline angle and cone angle of the SPS force as a function of θ_i .

of the momentum transported by the incident radiation are also shown. The x, z components and the modulus of \mathbf{D} are reported in Fig. 3(c), and $|\mathbf{D}|$ can be compared with the change of PMV calculated in the case of an ideal sail able to reflect 100% of the incoming radiation. Due to the intrinsic absorption of the aluminum film, the sail thrust loses approximately 0.35 μPa for $\theta_i = 0^\circ$ in comparison with the ideal case. This value is indeed -7.7% of the ideal thrust, quite a non-negligible amount in SPS trajectory computation [4]. Furthermore, for the same reason, \mathbf{D} is not aligned with the sail normal $\hat{\mathbf{m}}$, as instead happens in the ideal case. The angle θ_D between \mathbf{D} and the sail normal is reported in Fig. 3(d) as a function of θ_i together with the so-called cone angle (θ_C) [25]. A pitch angle above 45° leads to a large deviation of the SPS force from $-\hat{\mathbf{m}}$, and as shown from the behavior of the cone angle, the force cannot be directed more than 60° away from the Sun line. This limitation, on the force direction, as is well known, poses constraints on the SPS trajectory [2,3].

In this case, \mathbf{D} can be calculated by using the $r_s(\theta_i)$ of the sail because it is simple to derive,

$$D_x(\theta_i) = -\frac{\text{BSI}}{c}[1 - r_s(\theta_i)] \sin(\theta_i), \quad (13)$$

$$D_z(\theta_i) = \frac{\text{BSI}}{c}[1 + r_s(\theta_i)] \cos(\theta_i), \quad (14)$$

$$-\theta_D = \arctan \left(\frac{1 - r_s(\theta_i)}{1 + r_s(\theta_i)} \tan(\theta_i) \right). \quad (15)$$

In practice, for a smooth sail, the photon momentum responsible for the solar sail thrust is easily estimated experimentally. By measuring the optical functions $n(\lambda)$ and $k(\lambda)$, $R_s(\theta_i, \lambda)$ is computed by means of the Fresnel equations, Eq. (A8). For a given solar irradiance and by means of Eq. (12), the photon momentum change is computed by means Eqs. (13) and (14). The tiring task is measuring the optical properties in the spectral range from 200 nm up to 20,000 nm by a combination of ellipsometer, spectrophotometer, and Fourier transform infrared spectroscopy (FTIR) measurements for different angles in order to resolve the optical functions in this wide wavelength range. Since in this case $a = 1 - r_s$, centerline angle θ_D depends on the absorptance; if this one increases, then a larger θ_D angle is derived. This subject will be developed starting in the next section.

4. ABSORPTANCE OF A QUASI-SMOOTH SPS

If the sail surface is rough, then a fraction of the incoming radiation is reflected in the specular direction while the remaining light is diffused in the hemisphere. For this reason, the *directional spectral hemispherical reflectance* $R_T(\lambda, \theta_i)$ has to be introduced because the total reflected radiation is due to the contribution of spectral specular reflectance R_S and *directional spectral hemispherical diffuse reflectance* $R_D(\lambda, \theta_i)$. By using \tilde{z} as a parameter for assessing roughness,

$$R_T(\lambda, \theta_i, \tilde{z}) = R_S(\lambda, \theta_i, \tilde{z}) + R_D(\lambda, \theta_i, \tilde{z}). \quad (16)$$

Moreover, roughness induces an absorption that adds to the intrinsic absorption of the surface material. Since the sail's reflective layer is not transparent, the conservation of energy per unit time entails

$$R_T(\lambda, \theta_i, \tilde{z}) + A(\lambda, \theta_i, \tilde{z}) = 1. \quad (17)$$

The fraction of radiation totally reflected by the sail can be estimated by knowing the absorptance of a rough sail. Equation (1) can be used to get R_D and R_S .

In order to introduce the model used in the following sections, a brief review is explained on the statistics used to manage the height profile of a surface. A rough surface can be described by three more relevant statistical functions. The 2D surface profile $\zeta(x, y)$ gives the heights' distribution. In the case of a Gaussian distribution of heights, the rms roughness \tilde{z} is the standard deviation of this distribution. By means of the same $\zeta(x, y)$ and the lagged profiles $\zeta(x + \tau_x, y + \tau_y)$, the surface autocorrelation function $\mathbb{C}(x, y, \tau_x, \tau_y)$ can be defined (see p. 40 in Ref. [10]). If the mean value of the profile $\langle \zeta(x, y) \rangle = 0$, $\mathbb{C}(x, y, \tau_x, \tau_y)$ agrees with the statistical autocovariance function ACV(τ_x, τ_y) of $\zeta(x, y)$. In the case of a random profile, ACV is a Gaussian function too,

$$\text{ACV}(\tau) = \tilde{z}^2 \exp[-(\tau^2/\ell^2)], \quad (18)$$

where $\tau = \sqrt{\tau_x^2 + \tau_y^2}$ and ℓ is the autocorrelation length of surface. The Fourier transform of $\mathbb{C}(x, y, \tau_x, \tau_y)$ is the power spectral density (PSD; f_x, f_y), which is again a Gaussian function,

$$\text{PSD}(f) = \pi \ell^2 \tilde{z}^2 \exp[-(\pi \ell f)^2], \quad (19)$$

$$\text{where } f = \sqrt{f_x^2 + f_y^2}.$$

Although there are fractal, exponential, and Lorentzian PSD functions used in the literature [10], in this work only the Gaussian PSD is considered. The two parameters for defining the surface statistics function are hence \tilde{z} and ℓ .

For calculating the absorptance as a function of roughness, a VST is employed belonging to the set of small perturbation methods (SPM), which requires that $\tilde{z} \ll \lambda$. In Elson and Sung's work [26], the absorptance is computed starting by the electric field inside the metallic surface with the right boundary conditions [27,28]. The total spectral absorptance $A = A_i + A_r$ is given by the intrinsic absorptance A_i , related to the unperturbed electrical field E_0 and by A_r , related to the perturbed E_1 produced by the surface roughness. The calculation takes in account the s and p polarizations of the incident light, whereas surface and roughness enter in the PSD. The explicit expressions of A_i and A_r are given in Eqs. (A15) and (A20) in Appendix A. In this way, $A(\lambda, \theta_i)$ and $R_T(\lambda, \theta_i) = 1 - A$ as a function of roughness can be computed.

The solar directional total absorptance of a quasi-smooth sail was computed for different surface parameters. In particular, $0.5 \text{ nm} \leq \tilde{z} \leq 2.5 \text{ nm}$ and $250 \text{ nm} \leq \ell \leq 5000 \text{ nm}$. The values chosen for \tilde{z} are motivated by the range of validity of the SPM theory used for the computation of the momentum of diffused photons and discussed in the next section. The \tilde{z} values used in our computations can be referred at an aluminum film similar to Al coated on a quartz substrate [29]. Conversely, bulk aluminum after a lapping process would have a surface roughness with \tilde{z} at least ten times larger [30,31]. Results have been analyzed by considering the relative difference,

$$\frac{\Delta a}{a} = \frac{a(\theta_i, \tilde{z}, \ell) - a_{\text{int}}(\theta_i)}{a(\theta_i, \tilde{z}, \ell)}, \quad (20)$$

where $a_{\text{int}}(\theta_i)$ is the *solar directional total intrinsic absorptance*. Figure 4 reports $\frac{\Delta a}{a}$ as computed by means of Eqs. (A15) and (A20) for SPS with different roughnesses. The relative mean absorptance increases, as expected, for larger \tilde{z} . Although the effect of the roughness on the absorption is not very large, it increases the absorptance more than 0.1% even for a rms roughness of 0.25 nm. Although an increase of 0.1% in the total solar absorptance appears negligible, its effects over the time gives a considerable error in the prediction of the actual spacecraft trajectory [32] (see Conclusions).

Absorptance increases on the incident angle, and for θ_i close to the pseudo-Brewster angle, a significant rise in $a(\theta_i)$ is observed as \tilde{z} increases. If different correlation lengths are considered, the behavior of $a(\theta_i)$ is not similarly intuitive, as shown by considering ever larger \tilde{z} . The absorptance curves computed for $250 \text{ nm} \leq \ell \leq 5000 \text{ nm}$ of a SPS with $\tilde{z} = 2.5 \text{ nm}$ are shown in Fig. 4(b). This case corresponds to a largest roughness considered in this work. At low incident angles, the absorptance at shorter correlation length can be larger than the computed a at longer ℓ . This occurs for any \tilde{z} considered in this work. Moreover, as θ_i increases, there is a reversal and a again appears to increase on ℓ . As a consequence, at low pitch angles, a SPS

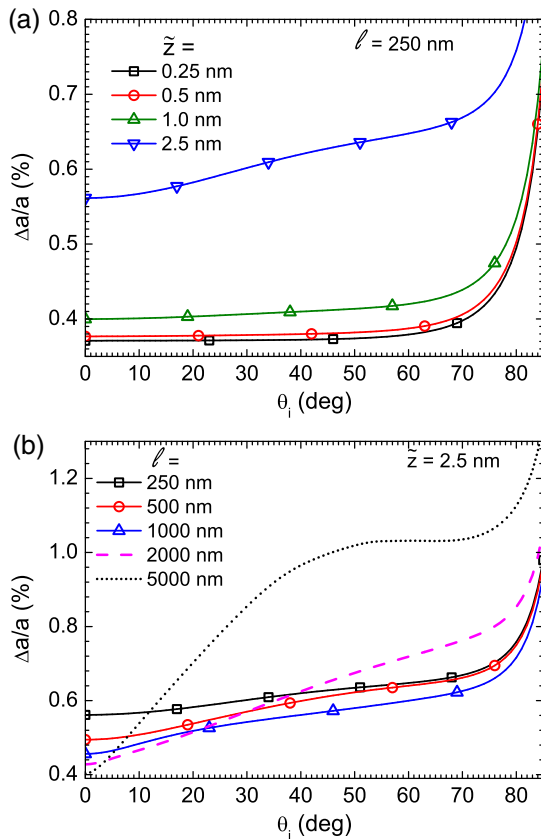


Fig. 4. (a) Relative mean total absorptance $\Delta a/a$ as a function of θ_i for different $0.25 \leq \tilde{z} \leq 2.5 \text{ nm}$ and $\ell = 250 \text{ nm}$. (b) $\Delta a/a$ of a sail with $\tilde{z} = 2.5 \text{ nm}$ but with different correlation lengths.

with a longer correlation length absorbs less photons than a sail with the same \tilde{z} but at shorter ℓ .

5. PHOTON MOMENTUM OF A QUASI-SMOOTH SPS

The next step is the estimation of R_D and BRDF of diffusing fraction of reflected light (BRDF_D), which could be computed by using the RRT, as effectively proposed by Vulpetti [16,33], who first used this theory for the computation of SPS photon momentum. Nevertheless, the RRT belongs at SPM class and only the second-order term of the series expansion is usually used since higher orders are very hard to manage. RRT series expansion converges quickly only for a very smooth surface. For the first perturbative term, the domain of validity is determined by the following criterion:

$$c_{RR} = (4\pi \cos \theta_i \tilde{z}/\lambda)^2 < 0.01. \quad (21)$$

This condition is derived by considering the case of a diffracting grating where a formal solution exists. Since the solar irradiance starts to be non-negligible at 200 nm, if $\theta_i = 0$, the condition in Eq. (21) is verified throughout if $\tilde{z} < 2.53 \text{ nm}$. This limit is stretched at larger \tilde{z} for larger θ_i . For example, for $\theta_i = 45^\circ$ (which is considered a large incident angle for a SPS mission), \tilde{z} can be 5.07 nm. For the range of \tilde{z} considered in this work, the ratio $\tilde{z}/\lambda \ll 1$ for any $200 \text{ nm} \leq \lambda \leq 20000 \text{ nm}$. In particular, for $\tilde{z} = 2.5 \text{ nm}$, $\tilde{z}/\lambda = 0.0125$ whenever $\lambda = 200 \text{ nm}$, and it decreases down to $\tilde{z}/\lambda = 0.000125$ as $\lambda = 20000 \text{ nm}$.

The first term of the RRT relates the optical properties to the morphological feature of the surface. The optical properties are described by the BRDF [19], while the morphological properties are set out by PSD [10]. For $\ell \gg \tilde{z}$,

$$\text{BRDF}_D(\lambda, \theta_i, \theta_s, \phi_s) = \frac{16\pi^2}{\lambda^4} \cos \theta_i \cos \theta_s Q \text{ PSD}(f_x, f_y). \quad (22)$$

The polarization factor Q does not depend on the surface morphology but just on the intrinsic optical properties of the material constituting the surface of the sail via the complex dielectric function $\epsilon(\lambda)$. Moreover, Q depends on θ_i , θ_s , ϕ_s . For each combination of the polarization of source and polarization of reflected beam, there are different Q terms, i.e., Q_{ss} , Q_{sp} , Q_{ps} and Q_{pp} [see Appendix A, Eq. (A9) for the expressions of the different terms]. Since the Sun is an unpolarized source and SPS does not select a particular polarization, $Q = 0.5(Q_{ss} + Q_{sp} + Q_{ps} + Q_{pp})$. For $\phi = 0$ and $\theta_s = \theta_i$, $Q_{ss}(\theta_i, \theta_i)$ and $Q_{pp}(\theta_i, \theta_i)$ reduce to Fresnel relations, whereas $Q_{sp}(\theta_i, \theta_i) = Q_{ps}(\theta_i, \theta_i) = 0$.

Spatial frequency f is obtained from hemispherical grating equations [10],

$$f_x = \frac{\sin \theta_s \cos \phi_s - \sin \theta_i}{\lambda}, \quad (23)$$

$$f_y = \frac{\sin \theta_s \sin \phi_s}{\lambda}. \quad (24)$$

In the literature, different VST theories can be found that could be used for surfaces with larger values of the \tilde{z}/λ ratio, but most of them are computationally intensive [34]. In particular,

promising results are obtained by using a phase perturbation theory [35–37]; nevertheless, the computations of the momentum of diffused photons are based on RRT in this work because (i) the expression of the RR's BRDF can be split into four clear pieces when the sail's surface roughness is sufficiently low; (ii) the multiple integrals giving the total photon momenta (per unit time and unit surface) reflected by the sail surface are all straightforward functions of the RR-VPT BRDF; (iii) the polarization factor and PSD are derived by a measurable quantity and they enter directly in the BRDF expression; and (iv) RR-VPT would allow us to deal with the inverse scattering problem (ISP) related to the navigation, guidance, and control subsystems.

From BRDF_D given by RRT, the \mathbf{D}_{rd} , R_D , can be computed by using

$$\mathbf{D}_{rd} \equiv \frac{1}{c} \int_{\lambda_{\min}}^{\lambda_{\max}} I(\lambda) d\lambda \int_{\Omega_s} \cos \theta_s \text{BRDF}_D \hat{\mathbf{d}}_s d\Omega_s, \quad (25)$$

$$R_D(\lambda, \theta_i, \tilde{z}, \ell) = \int_{\Omega_s} \text{BRDF}(\theta_s \neq \theta_i) \cos \theta_s d\Omega_s. \quad (26)$$

At the same time, *solar directional total hemispherical diffuse reflectance* r_d can be defined as

$$r_d(\theta_i) = (1/\text{BSI}) \int_{\lambda_{\min}}^{\lambda_{\max}} R_D(\lambda, \theta_i) I(\lambda) d\lambda. \quad (27)$$

$R_S(\lambda, \theta_i, \tilde{z}, \ell)$ is given by $R_T - R_D$, hence obtaining the BRDF_S given by Eq. (11). Photon momentum due to the specular beam (\mathbf{D}_{rs}) is given by

$$\mathbf{D}_{rs} \equiv \frac{1}{c} \int_{\lambda_{\min}}^{\lambda_{\max}} I(\lambda) d\lambda \int_{\Omega_s} \cos \theta_s \text{BRDF}_S \hat{\mathbf{d}}_s d\Omega_s, \quad (28)$$

In this way, the \mathbf{D} of SPS can be estimated by Eq. (7), accounting for $\mathbf{D}_r = \mathbf{D}_{rs} + \mathbf{D}_{rd}$.

For computing one point of a curve, first it is necessary to specify \tilde{z} , ℓ , and θ_i values. θ_i is discretized by considering a step of 1 deg in the range $0 \leq \theta_i \leq 90$, whereas θ_s and ϕ_s are discretized with a vector of $N = 180$ elements. In this way, $\hat{\mathbf{d}}_s$, $\hat{\mathbf{d}}_i$ are straightforwardly discretized. The Sun irradiance used is the Solar Spectra Air Mass Zero (AM0) of ASTM E490 (1974–2000), and it is discretized on λ considering a 1 nm step within $200 \text{ nm} \leq \lambda \leq 20,000 \text{ nm}$. The experimental complex $\epsilon(\lambda)$ is also a vector with 19,801 components obtained by discretizing the experimental optical indexes of a thin aluminum film 100 nm thick. The spectral optical quantities, such as $R_D(\lambda, \theta_i)$, are hence discretized as matrices of $19,801 \times 91$ elements.

A loop that changes λ value allows us to compute BRDF at each step of 1 nm. For any λ value assumed in the loop, f , PSD, and Q are matrices of $N \times N = 180$ obtained by using the discretized θ_s and ϕ_s . Finally, by a straightforward matrix algebra, the BRDF is computed. All the integrals needed for calculating momenta and optical quantities are computed via the Simpson rule with 2D or 3D integration according to the physical quantity.

In Fig. 5, r_s and r_d are shown as a function of θ_i for SPS with $\tilde{z} = 2.5 \text{ nm}$ and different values of ℓ . This is the largest \tilde{z} used for which $c_{RR} < 0.01$ for any λ in $I(\lambda)$. In the same graph, the r_s of an ideal smooth sail is reported, and its value differs from

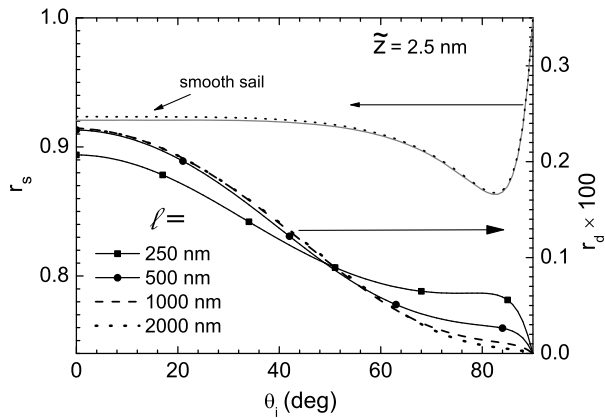


Fig. 5. Solar directional total specular reflectance (r_s) and solar directional total hemispherical diffuse reflectance (r_d) as a function of θ_i of SPSs with $\tilde{z} = 2.5 \text{ nm}$ and $250 \text{ nm} \leq \ell \leq 2000 \text{ nm}$.

the computed curve via RRT less than 1%. In the same panel, r_d curves are also shown but points are magnified to 100 times the actual values. Despite little light being widespread for this \tilde{z} , there is a clear dependence of r_d on ℓ . In the two panels of Fig. 6, the x component (lower panel) and z component (upper panel) of the PM arisen by diffuse radiation are also

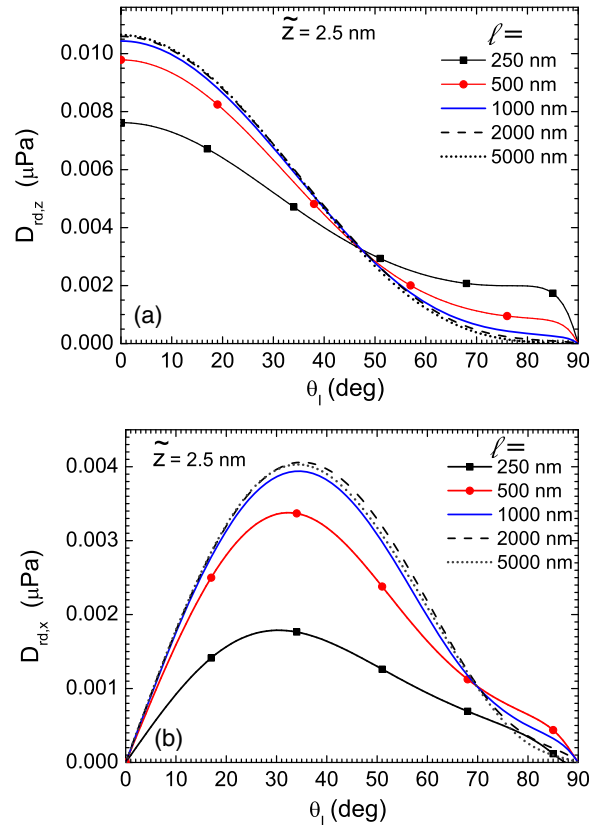


Fig. 6. Normal component of the photon momentum of the diffuse radiation $D_{rd,z}$ (upper panel) and in plane component $D_{rd,x}$ (lower panel) versus θ_i of SPSs with $\tilde{z} = 2.5 \text{ nm}$ and $250 \text{ nm} \leq \ell \leq 5000 \text{ nm}$.

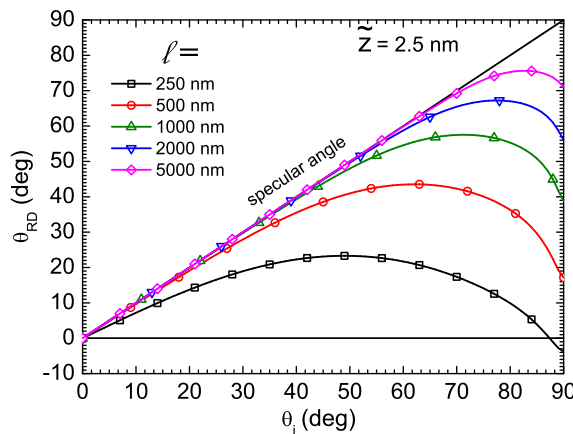


Fig. 7. Angle θ_{rd} , formed by \mathbf{D}_{rd} with $\hat{\mathbf{m}}$ as a function of (θ_i) of SPSs with $\tilde{z} = 2.5 \text{ nm}$ and $250 \text{ nm} \leq \ell \leq 5000 \text{ nm}$.

shown. The maximum value of $\mathbf{D}_{rd} = 0.012 \mu\text{Pa}$ results for $\ell > 2000 \text{ nm}$.

The most important outcome of \mathbf{D}_{rd} dependence on the coherence length is shown in Fig. 7, where the angle θ_{rd} between \mathbf{D}_{rd} and $\hat{\mathbf{m}}$ is shown as a function of θ_i for different ℓ . The vector \mathbf{D}_{rd} is not aligned along the SPS normal as usually assumed in most employed thrust models [6]. As shown in Fig. 7, the θ_{rd} depends largely on ℓ . In particular, for shorter ℓ , where a lower scattering is observed, a larger deviation of the scattered halo from the specular direction results. In contrast, longer ℓ leads to having \mathbf{D}_{rd} point along the specular directions due to the diffuse photons, except for very large pitch angles.

As a consequence, diffuse momentum computed via RRT affects the PMV given by Eq. (7). The reduction of its intensity and the resulting centerline angle (θ_D) depends on θ_i as well as on SPS surface statistical parameters. In Fig. 8(a), the difference between the module of the PMV of a quasi-smooth sail and the momentum change of an ideally smooth SPS, named ΔD , is reported as a function of θ_i . Figure 8(a) shows only computations obtained for $\tilde{z} = 2.5 \text{ nm}$ but for different ℓ . The behavior is not straightforward. The largest difference with the \mathbf{D} computed in the smooth case is obtained for a SPS with $\ell = 250 \text{ nm}$. Although for this ℓ the r_d shown in Fig. 5(a) is the weakest, the absorption for $\theta_i < 40^\circ$ is the largest if it is compared with the longer ℓ . Moreover, θ_{rd} strays further from the specular direction, and this is detrimental for \mathbf{D} . For $\theta_i > 40^\circ$, the trend is overturned, and (ΔD) is now larger for the shortest ℓ considered in our computation. In this case, it is due to a larger z component of the relative \mathbf{D}_{rd} compared with the other ones for longer ℓ . Furthermore, \mathbf{D} is higher than the PMV change computed in a smooth SPS, starting from $\theta_i \approx 64^\circ$. This can be explained by noticing that the z component of \mathbf{D}_{rd} is almost constant, whereas $D_{r,z}$ of a smooth SPS, shown in Fig. 3(b), decreases on θ_i .

For $\tilde{z} = 2.5 \text{ nm}$, ΔD is less than $5 \times 10^{-3} \mu\text{Pa}$, but this value cannot be neglected, and it is expected to increase at larger roughnesses.

On the other hand, the deviation of the \mathbf{D} direction far from $\hat{\mathbf{m}}$, given by the θ_D angle, is shown in Fig. 8(b) as $\Delta\theta_D = \theta_D(\tilde{z} = 0) - \theta_D(\tilde{z})$. It is clarified that θ_D is the angle

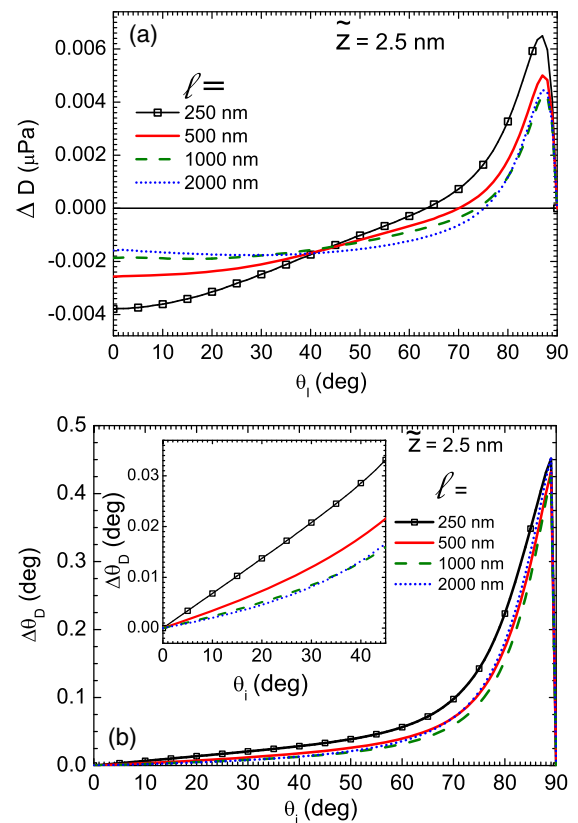


Fig. 8. Computed data reported in the two panels are referred at SPS with $\tilde{z} = 2.5 \text{ nm}$ and $250 \text{ nm} \leq \ell \leq 2000 \text{ nm}$. (a) ΔD as a function of the pitch angle computed by using RRT and the PM change of the smooth case. (b) Change of the centerline angle with respect to the smooth case, $\Delta\theta_D$. In the inset of (b), a zoom of $\Delta\theta_D$ for $\theta_i \leq 45^\circ$.

formed by \mathbf{D} with $\hat{\mathbf{m}}$, and in our convention, a positive angle is measured starting from $\hat{\mathbf{m}}$ and rotating clockwise. $\Delta\theta_D$ increases with θ_i , and the largest deviation between \mathbf{D} and $\hat{\mathbf{m}}$ occurs, as expected, for the shortest ℓ considered. However, for the set of surface parameters considered up to now, θ_D remains in the order of 10^{-1} deg away from θ_D for a smooth SPS. In particular, as shown in the inset of Fig. 8(b), such deviation is in the order of 10^{-2} deg for $\theta_i \leq 45^\circ$ deg. As a consequence, there is not a significant effect on the direction of SPS force due to the diffuse radiation for values of \tilde{z} where RRT can be applied. Nevertheless, a tenth of a degree produces a large change of SPS effective flight, especially if a mission—as an example, toward the Kuiper Belt—was planned.

6. CONCLUSIONS

In this paper, the PMV change, which is the source of SPS thrust, is analyzed. Although the main focus of this paper seems to be connected to an aerospace engineering topic, the subject is dealt with from a point of view closer to light scattering and photon momentum. Usually, in the optics literature, spectral optical quantities are considered by focusing on a material or device's behavior. In addition, if the scattering is the focus, BRDF curves, restricted to the plane of incidence

and for a discrete number of wavelengths, are discussed. For evaluating SPS thrust, the BRDF on the whole hemisphere has to be taken into account in a wide wavelength band of the full solar spectral irradiance, because the sails' BRDF has to be integrated over such band for calculating the result of the reflected photons momenta. RRT allows computation of the momentum due to diffuse photons. At the same time, the momentum of the specularly reflected photons can be evaluated if the SPS absorptance, depending also on roughness, is also computed. To such an aim, SPM theories of scattering can be successfully used for computing \mathbf{D} and all the spectral optical features, provided that the sail surface is quasi-smooth. Absorptance of the metallic layer primarily determines the angle θ_D formed by the PMV change with \hat{m} , even in the smooth SPS. PMV depends on \tilde{z}^2 , but the most interesting results are related to its dependence on ℓ . In particular, the correlation length affects the direction of \mathbf{D}_{rd} . Shorter ℓ values induce resulting scattered momenta farther from the surface normal, but with an angular lag with respect to the specular reflection (especially for large incidence angles). All the results discussed in this work show that it is possible to determine with high accuracy the force acting on an aluminum-coated space sail if its surface roughness satisfies the ratio $\tilde{z}/\lambda \leq 1/100$. On the other hand, solar-sailing propulsion by means of somewhat rough sails would be decreased in performance because of the restricted class of viable space missions coming from (1) the decreased thrust acceleration magnitude and (2) the narrow range of control of the thrust direction. In contrast, if the sail is sufficiently smooth, quite new scenarios of space sailing open up.

A criticism can be expressed due to the small variations obtained in the calculated physical quantities if they are compared with the ideal smooth case. Nevertheless, for instance, sailcraft acceleration at ~ 1 AU is sensitive to changes of the order of 4 nPa in radiation pressure; ensuing trajectory velocity errors accumulate as (flight) time goes by. Equivalently, in an optical model of thrust, if one neglects wave–sail interaction effects of this order or higher, then the (space) trajectory design may cause real off-nominal trajectory deviations too difficult to correct in flight because SPS is a low-acceleration propulsion. A good sailcraft trajectory design should include prediction of flight errors rectifiable by the devised navigation, guidance, and control subsystems, which therefore will have to contain a good model of thrust. The plots in Fig. 8 should be read in this sense: diffuse reflection is equivalent to 1–10 nPa. To conclude, if the diffuse radiation of a quasi-smooth surface can be neglected in most optical applications, the same concept could not be brought into photon sailing [32,38,39].

APPENDIX A

In order to make the reading easier, let us first report the expressions of the Fresnel reflectance, the polarization factors for non-magnetic metals, and the two types of absorptance.

A. Fresnel Equations for Reflectance

Let us define the following identities:

$$q_i = \cos \theta_i, \quad (\text{A1})$$

$$q_s = \cos \theta_s, \quad (\text{A2})$$

$$k_i = \sin \theta_i, \quad (\text{A3})$$

$$k_s = \sin \theta_s, \quad (\text{A4})$$

$$h_i = \sqrt{\epsilon - \sin^2 \theta_i}, \quad (\text{A5})$$

$$h_s = \sqrt{\epsilon - \sin^2 \theta_s}, \quad (\text{A6})$$

where the dielectric complex function ϵ depends on λ and is related to refracting index n and extinction coefficient k from

$$\epsilon = \epsilon_1 + i\epsilon_2 = n^2 - k^2 + i2nk. \quad (\text{A7})$$

The “directional” spectral specular reflectance of a smooth surface $R_{S,0}$ is given by

$$R_{S,0}(\lambda, \theta_i) = \frac{1}{2} \left[\left| \frac{q_i - h_i}{q_i + h_i} \right|^2 + \left| \frac{\epsilon q_i - h_i}{\epsilon q_i + h_i} \right|^2 \right], \quad (\text{A8})$$

where the subscript “0” is for stressing that the formula refers to the spectral specular reflectance of a smooth surface.

B. Q Polarization Factor

The BRDF of RRT depends on Q [40,41], which is a real number depending on the complex permeability of the materials as well as the incident and scattering angles. Moreover, Q is actually the sum of four different terms related to the four different combinations of polarizations of the incident and scattered beam (i.e., ss , sp , ps , pp). The final Q value depends on the polarization of the source and detector. For the sail system, the source is unpolarized, and the emerging beam is composed of the s - and p -polarized light. For this reason,

$$Q = \frac{1}{2} (Q_{ss} + Q_{sp} + Q_{ps} + Q_{pp}), \quad (\text{A9})$$

and the polarization factors for the four different polarizations are given by

$$Q_{ss} = \left| \frac{(\epsilon - 1) \cos \phi_s}{(q_i + h_i)(q_s + h_s)} \right|^2, \quad (\text{A10})$$

$$Q_{sp} = \left| \frac{(\epsilon - 1) h_s \sin \phi_s}{(q_i + h_i)(\epsilon q_s + h_s)} \right|^2, \quad (\text{A11})$$

$$Q_{ps} = \left| \frac{(\epsilon - 1) h_i \sin \phi_s}{(\epsilon q_i + h_i)(q_s + h_s)} \right|^2, \quad (\text{A12})$$

$$Q_{pp} = \left| \frac{(\epsilon - 1)(h_s h_i \cos \phi_s - \epsilon k_i k_s)}{(\epsilon q_i + h_i)(\epsilon q_s + h_s)} \right|^2. \quad (\text{A13})$$

C. Absorptance of a Rough Surface

The absorptance, i.e., the ratio of absorbed energy to incident energy, is given by [26]

$$A = A_i + A_r, \quad (\text{A14})$$

where the intrinsic absorptance A_i is given by

$$A_i = \frac{2q_i \epsilon_2}{\text{Im}(h_i)} \left[\frac{k_i^2 + |h_i|^2}{|h_i + \epsilon q_i|^2} + \frac{1}{|h_i + q_i|^2} \right]. \quad (\text{A15})$$

The absorptance due to the surface roughness (A_r) is obtained by means of the first-order solution of the perturbed electrical field both for s - and p -polarized light beams with the condition $\tilde{z} \ll \lambda$. By letting

$$\mathbf{k} = k(\hat{x} \cos \phi + \hat{y} \sin \phi), \quad (\text{A16})$$

$$\mathbf{k}_i = k_i \hat{x}, \quad (\text{A17})$$

$$h = \sqrt{\epsilon - k^2}, \quad (\text{A18})$$

$$q = \sqrt{1 - k^2}, \quad (\text{A19})$$

$$A_r = \frac{\epsilon_2 |\epsilon - 1| q_i}{2\pi^2} \int \left(\frac{2\pi}{\lambda} \right)^4 d^2k \left\{ \text{PSD} \left[\frac{2\pi}{\lambda} (\mathbf{k} - \mathbf{k}_i) \right] \frac{1}{\text{Im}(h)} \times \left[\frac{(k^2 + |h|^2)}{|h + eq_i|^2} \left| \frac{(h_i q \cos \phi + kk_i)}{\epsilon q_i + h_i} + \frac{q \sin \phi}{q_i + h_i} \right|^2 + \frac{1}{|q + h|} \left| \frac{\cos \phi}{q_i + h_i} + \frac{h_i \sin \phi}{\epsilon q_i + h_i} \right|^2 \right] \right\}. \quad (\text{A20})$$

Funding. ENEA, National Agency for New Technologies, Energy and Sustainable Economic Development; Sapienza Università di Roma, Italy.

Acknowledgment. This work has been motivated by several discussions with Giulio Maddalena, Federica Bonetti, Mattia Carosi, and Valentina Macchiarulo, during the tutoring of their master's theses. The authors also thank Dr. Rosa Chierchia for her useful comments and suggestions.

REFERENCES AND NOTES

- J. D. Acord and J. C. Nicklas, *Theoretical and Practical Aspects of Solar-Pressure Attitude Control for Interplanetary Spacecraft, Guidance and Control II* (Academic, 1994).
- J. L. Wright, *Space Sailing* (Gordon and Breach Science, 1992).
- C. R. McInnes, *Solar Sailing: Technology, Dynamics, and Mission Applications* (Springer-Verlag Berlin, 1999).
- G. Vulpetti, *Fast Solar Sailing, Space Technology Library* (Springer Netherlands, 2013), Vol. 30.
- W. Seboldt and B. Dachwald, "Solar sails for near term advanced scientific deep space missions," in *Proceedings of 8th International Workshop on Combustion and Propulsion*, Pozzuoli (NA), Italy, 2002.
- B. Fu, E. Sperber, and F. Eke, "Solar sail technology a state of the art review," *Prog. Aero. Sci.* **86**, 1–19 (2016).
- H. Spencer and A. C. Kieran, "Real solar sails are not ideal, and yet it matters," in *Advances in Solar Sailing*, M. Macdonald, ed. (Springer Berlin Heidelberg, 2014), Vol. 14, pp. 25–43.
- H. Davies, "The reflection of electromagnetic waves from a rough surface," *Proc. IEE Pt. III* **101**, 209–214 (1954).
- H. E. Bennet and J. O. Porteu, "Relation between surface roughness and specular reflectance at normal incidence," *J. Opt. Soc. Am.* **51**, 123–129 (1961).
- J. C. Stover, *Optical Scattering: Measurement and Analysis*, 3rd ed. (SPIE, 2012), vol. PM224.
- G. Vulpetti and S. Scaglione, "The AURORA project: estimation of the optical parameters," *Acta Astronaut.* **48**, 123–132 (1999).
- In this work, the angle θ_i is the angle between the SPS normal and the direction of the Sun. The usual nomenclature used in aerospace defines this angle as pitch angle.
- G. Mengali and A. A. Quarta, "Optimal three-dimensional interplanetary rendezvous using nonideal solar sail," *J. Guid. Control. Dyn.* **28**, 173–177 (2005).
- G. Mengali, A. A. Quarta, C. Circi, and B. Dachwald, "Refined solar sail force model with mission application," *J. Guid. Control. Dyn.* **30**, 512–520 (2007).
- S. O. Rice, "Reflection of electromagnetic waves from slightly rough surfaces," *Commun. Pure Appl. Math.* **4**, 351–378 (1951).
- G. Vulpetti, "Applying vector scattering theory to solar-photon sail thrust modeling," in *Advances in Solar Sailing*, M. Macdonald, ed., Springer Praxis Books (Springer Berlin Heidelberg, 2014), pp. 489–508.
- In this work, PMV is discussed instead the SPS momentum, which has only an opposite orientation.
- C. A. Gueymard, "The Sun's total and spectral irradiance for solar energy applications and solar radiation models," *Sol. Energy* **76**, 423–453 (2004).
- F. E. Nicodemus, J. C. Richmond, J. J. Hsia, I. Ginsber, and T. Limperis, *Geometric Considerations and Nomenclature for Reflectance*, NBS Monograph (U.S. Dept of Commerce, 1977), Vol. 160, p. 1.
- The used values of TSI and BSI are related to the TSI composite relative to the previous solar cycles (we now are in solar cycle 24). Recent and more reliable TSI time series have been coming from the observations of the NASA/SORCE spacecraft, and they will be considered in a next paper.
- Solar Radiation and Climate Experiment (SORCE), <http://lasp.colorado.edu/home/sorce/>.
- G. P. Pells and M. Shiga, "The optical properties of copper and gold as a function of temperature," *J. Phys. C* **2**, 1835–1846 (1969).
- A. G. Mathewson and H. P. Myers, "Optical absorption in aluminium and the effect of temperature," *J. Phys. F* **2**, 403–415 (1972).
- J. M. Palmer, "The measurement of transmission, absorption, emission and reflection," in *Handbook of Optics*, M. Bass, ed., 2nd ed. (McGraw Hill, 1995), Vol. II, pp. 25.1–25.25, chap. 25.
- In the nomenclature used in aerospace literature, the cone angle is used instead of the centerline angle. Cone angle is defined as the angle between the SPS momentum and the specular direction. If cone angle is equal to θ , the SPS force is along \hat{m} , implying that the centerline angle is zero.
- J. M. Elson and C. C. Sung, "Intrinsic and roughness-induced absorption of electromagnetic radiation incident on optical surfaces," *Appl. Opt.* **21**, 1496–1501 (1982).
- E. Kröger and E. Kretschmann, "Scattering of light by slightly rough surfaces or thin films including plasma resonance emission," *Z. Phys.* **237**, 1–15 (1970).
- A. Marvin, F. Toigo, and V. Celli, "Light scattering from rough surfaces: general incidence angle and polarization," *Phys. Rev. B* **11**, 2777–2782 (1975).
- K. H. Guenther, P. G. Wierer, and J. M. Bennett, "Surface roughness measurements of low-scatter mirrors and roughness standards," *Appl. Opt.* **23**, 3820–3836 (1984).
- H. Fujii and T. Asakura, "Roughness measurements of metal surfaces using laser speckle," *J. Opt. Soc. Am.* **67**, 1171–1176 (1977).
- R. C. Birkebak and E. R. G. Eckert, "Effects of roughness of metal surfaces on angular distribution of monochromatic reflected radiation," *J. Heat Transfer* **87**, 85–94 (1965).
- G. L. Matloff, G. Vulpetti, C. Bangs, and R. Haggerty, "The interstellar probe (ISP): pre-perihelion trajectories and application to holography," *Tech. Rep. NASA/CR-2002-211730* (NASA, 2002).
- G. Vulpetti, L. Johnson, and G. L. Matloff, *Solar Sails: A Novel Approach to Interplanetary Travel*, 2nd ed. (Springer, 2015).
- T. M. Elfouhaily and C.-A. Guérin, "A critical survey of approximate scattering wave theories from random rough surfaces," *Wave Random Media* **14**, R1–R40 (2004).
- A. G. Navarrete Alcalá, E. I. Chaikina, E. R. Méndez, T. A. Leskova, and A. A. Maradudin, "Specular and diffuse scattering of light from two-dimensional randomly rough metal surfaces: experimental and theoretical results," *Waves Random Complex Media* **19**, 600–636 (2009).
- I. Simonsen, A. A. Maradudin, and T. A. Leskova, "Scattering of electromagnetic waves from two-dimensional randomly rough perfectly

- conducting surfaces: the full angular intensity distribution," *Phys. Rev. A* **81**, 013806 (2010).
37. A. A. Maradudin, T. Michel, A. R. McGurn, and E. R. Méndez, "Enhanced backscattering of light from a random grating," *Ann. Phys.* **203**, 255–307 (1990).
38. G. Vulpetti, "Effect of the total solar irradiance variations on solar-sail low-eccentricity orbits," *Acta Astronaut.* **67**, 279–283 (2010).
39. G. Vulpetti, "Total solar irradiance fluctuation effects on sailcraft-Mars rendezvous," *Acta Astronaut.* **68**, 644–650 (2011).
40. E. L. Church and J. M. Zavada, "Residual surface roughness of diamond-turned optics," *Appl. Opt.* **14**, 1788–1795 (1975).
41. A. A. Maradudin and D. L. Mills, "Scattering and absorption of electromagnetic radiation by a seminfinite medium in the presence of surface roughness," *Phys. Rev. B* **11**, 1392–1415 (1975).